Discontinuous Galerkin Methods for Electromagnetic Waves in Dispersive Media

Thomas Hagstrom

Department of Mathematics

Southern Methodist University

Dallas TX, USA

thagstrom@smu.edu

Daniel Appelö

Department of Computational Mathematics,
Science & Engineering
Department of Mathematics
Michigan State University
East Lansing MI, USA
appeloda@msu.edu

Lu Zhang
Department of Applied Physics
and Applied Mathematics
Columbia University
New York NY, USA
1z2784@columbia.edu

Abstract—We consider numerical methods for Maxwell's equations in general linear dispersive media. First, we use standard energy techniques to prove stability for discontinuous Galerkin methods applied to both first-order and second-order formulations. Second, we discuss the general representation of the polarization kernel by rational functions in continued fraction form.

Index Terms—dispersive media, discontinuous Galerkin methods, rational approximation.

I. INTRODUCTION

We consider Maxwell's equations in an isotropic dispersive medium, written both as a first order system

$$\frac{\partial \mathbf{D}}{\partial t} = \nabla \times \mathbf{H} - \mathbf{J},
\frac{\partial \mathbf{H}}{\partial t} = -\frac{1}{\mu_0} \nabla \times \mathbf{E},
\nabla \cdot \mathbf{H} = 0, \quad \nabla \cdot \mathbf{D} = \rho,$$
(1)

and in second order form

$$\frac{\partial^2 \mathbf{D}}{\partial t^2} = -\frac{1}{\mu_0} \nabla \times \nabla \times \mathbf{E} - \frac{\partial \mathbf{J}}{\partial t},\tag{2}$$

where

$$\mathbf{D} = \epsilon_0 \mathbf{E} + \mathbf{P}. \tag{3}$$

Discontinuous Galerkin (DG) methods applied to (1) or (2) have a number of desirable features; they are geometrically flexible and can achieve aribitrary-order in a straightforward way. For applications to electromagnetic waves in dispersive media see [1] and references therein. Our goals are to analyze the stability of DG methods for a general linear polarization **P** and to describe effective methods for the localized reduced order modeling of **P**.

We note that the disadvantage of DG methods relative to alternative high-order schemes on structured grids such as [2], [3] is the excessive restriction on the time step for explicit schemes, worse by a factor of the polynomial degree. A possible approach to circumventing this restriction in cases where uniform media form a sufficiently large portion of the domain are to use either Galerkin difference [4]–[7] or staggered [8] formulations, but we will not consider these here.

II. LINEAR DISPERSION MODELS

Consider a general time-translation-invariant linear dispersion model taking the form of a temporal convolution:

$$\mathbf{P}(\mathbf{x},t) = \epsilon_0 \int_0^t \chi(\mathbf{x},\tau) \mathbf{E}(\mathbf{x},t-\tau) d\tau. \tag{4}$$

Here we will focus on the typical case where the convolution kernel χ is piecewise constant; that is only varying from material to material. We also note that in our notation ϵ_0 and μ_0 may also vary from material to material. To emphasize this we will drop the \mathbf{x} in describing χ , but will note the role of discontinuities at material interfaces when we discuss the DG discretizations. It is convenient to express the polarization using a Laplace transformation in time:

$$\hat{\mathbf{P}}(\mathbf{x}, s) = \epsilon_0 \hat{\chi}(s) \hat{\mathbf{E}}(\mathbf{x}, s). \tag{5}$$

We explicitly assume that $\hat{\chi}$ is analytic in $\Re s > 0$ and that it represents a lower order term in that $|\hat{\chi}| = O(s^{-1}), |s| \to \infty$. We also assume that χ satisfies the stability condition

$$\Re(s\hat{\chi}) > 0, \quad \Re s > 0. \tag{6}$$

An immediate consequence of (6) is an energy estimate for solutions of both the first and second order formulations. These follow from the positivity of convolutions with kernels satisfying (6) (e.g. [9, Ch. 16] and [10]). For any function u(t)

$$\int_{0}^{T} u(t) \left(\chi * \frac{du}{dt} \right) (t) dt \ge 0. \tag{7}$$

We first consider (1). Define, for any domain Ω

$$\mathcal{E}_1(t) = \frac{1}{2} \int_{\Omega} \epsilon_0 |\mathbf{E}|^2 + \mu_0 |\mathbf{H}|^2.$$

Then, differentiating in time and applying the standard arguments we find

$$\frac{d\mathcal{E}_{1}}{dt} = -\epsilon_{0} \int_{\Omega} \mathbf{E} \cdot \left(\chi * \frac{\partial \mathbf{E}}{\partial t} \right) - \int_{\Omega} \mathbf{E} \cdot \mathbf{J} + \int_{\partial \Omega} (\mathbf{H} \times \mathbf{E}) \cdot n. \tag{8}$$

Integrating in time and applying (7) component-wise we obtain an expression for $\Delta \mathcal{E}_1 = \mathcal{E}_1(t) - \mathcal{E}_1(0)$:

$$\Delta \mathcal{E}_1 \le -\int_0^t \left(\int_{\Omega} \mathbf{E} \cdot \mathbf{J} + \int_{\partial \Omega} \left(\mathbf{H} \times \mathbf{E} \right) \cdot n \right) dt. \tag{9}$$

Now consider (2). Define

$$\mathcal{E}_2(t) = \frac{1}{2} \int_{\Omega} \epsilon_0 |\frac{\partial \mathbf{E}}{\partial t}|^2 + \frac{1}{\mu_0} |\nabla \times \mathbf{E}|^2.$$

Then, again differentiating in time and applying the standard arguments we find

$$\frac{d\mathcal{E}_{2}}{dt} = -\int_{\Omega} \epsilon_{0} \frac{\partial \mathbf{E}}{\partial t} \cdot \left(\chi * \frac{\partial^{2} \mathbf{E}}{\partial t^{2}} \right)$$

$$-\int_{\Omega} \frac{\partial \mathbf{E}}{\partial t} \cdot \frac{\partial \mathbf{J}}{\partial t} - \int_{\partial \Omega} \frac{1}{\mu_{0}} \left((\nabla \times \mathbf{E}) \times \frac{\partial \mathbf{E}}{\partial t} \right) \cdot \mathbf{n}.$$
(10)

Integrating in time and applying (7) component-wise we now obtain:

$$\Delta \mathcal{E}_{2} \leq -\int_{0}^{t} \int_{\Omega} \frac{\partial \mathbf{E}}{\partial t} \cdot \frac{\partial \mathbf{J}}{\partial t} dt \qquad (11)$$
$$-\int_{0}^{t} \int_{\partial \Omega} \frac{1}{\mu_{0}} \left((\nabla \times \mathbf{E}) \times \frac{\partial \mathbf{E}}{\partial t} \right) \cdot \mathbf{n} dt.$$

We remark that in the absence of charges $\nabla \cdot \mathbf{E} = 0$ and (2) can be replaced by a standard vector wave equation, as used computationally in [3]. Then \mathcal{E}_2 can be replaced by the usual energy for the scalar wave equation applied component-wise and the boundary flux density replaced by $\nabla \mathbf{E} \cdot \frac{\partial \mathbf{E}}{\partial t}$.

III. DISCONTINUOUS GALERKIN DISCRETIZATIONS IN SPACE

Leaving time continuous, we consider the approximation of (1) or (2) by discontinuous Galerkin methods. Given the energy estimates listed above and the fact that the energy flux at boundaries is independent of the polarization model, these only require an addition of the polarization terms to approximations developed in the nondispersive case. Specifically we assume the domain Ω is divided into the union of nonoverlapping elements Ω_j and that the fields are approximated by piecewise polynomials relative to this partition. We will also assume that material boundaries coincide with element boundaries.

A. First Order Formulation

Approximating (1) follows the standard procedure outlined in [11]. On each element Ω_j we approximate \mathbf{E} , \mathbf{H} component-wise by polynomials of degree q, \mathbf{E}^h , \mathbf{H}^h , and impose for all component-wise degree q test functions Φ_E , Φ_H ,

$$\int_{\Omega_{j}} \phi_{E} \cdot \frac{\partial \mathbf{D}^{\mathbf{h}}}{\partial t} - \frac{1}{2} \left(\mathbf{\Phi}_{E} \cdot (\nabla \times \mathbf{H}^{\mathbf{h}}) + (\nabla \times \mathbf{\Phi}_{E}) \cdot \mathbf{H}^{h} \right)
= \int_{\partial \Omega_{j}} \left(\mathbf{n} \times \left(\mathbf{H}^{*} - \frac{1}{2} \mathbf{H}^{h} \right) \right) \cdot \mathbf{\Phi}_{E} - \int_{\Omega_{j}} \phi_{E} \cdot \mathbf{J},
\int_{\Omega_{j}} \mu_{0} \phi_{H} \cdot \frac{\partial \mathbf{H}^{\mathbf{h}}}{\partial t} + \frac{1}{2} \left(\mathbf{\Phi}_{H} \cdot (\nabla \times \mathbf{E}^{\mathbf{h}}) + (\nabla \times \mathbf{\Phi}_{H}) \cdot \mathbf{E}^{h} \right)
= \int_{\partial \Omega_{j}} \left(\mathbf{n} \times \left(\mathbf{E}^{*} - \frac{1}{2} \mathbf{E}^{h} \right) \right) \cdot \mathbf{\Phi}_{H}.$$

To facilitate the computation of \mathbf{P}^h we would generally use nodal degrees-of-freedom to represent the polynomials. In addition we have written down the partially integrated form which allows us to retain the energy estimates when exact integration is replaced by a numerical quadrature with positive weights. Then the integrals in the energy estimate are simply replaced by quadratures.

At interelement boundaries we can choose the standard fluxes [11], where the parameter α , $0 \le \alpha \le 1$, controls the upwinding and the outside states at physical boundaries are chosen to impose the boundary conditions. In these formulas + denotes the outside state, - denotes the inside state, $Z = Y^{-1} = \sqrt{\mu_0/\epsilon_0}$. Jumps in the material parameters are allowed with $\{W\} = (W^+ + W^-)/2$, [[W]] for W = Z, Y. The expressions for $\mathbf{n} \times \left(\mathbf{H}^* - \frac{1}{2}\mathbf{H}^h\right)$ and $\mathbf{n} \times \left(\mathbf{E}^* - \frac{1}{2}\mathbf{E}^h\right)$ are, respectively,

$$\begin{split} &\frac{1}{2\{Z\}}\mathbf{n}\times\left(Z^{+}\mathbf{H}^{h,+}+\frac{[[Z]]}{2}\mathbf{H}^{h}+\alpha\mathbf{n}\times\left(\mathbf{E}^{h}-\mathbf{E}^{h,+}\right)\right),\\ &\frac{1}{2\{Y\}}\mathbf{n}\times\left(Y^{+}\mathbf{E}^{h,+}+\frac{[[Y]]}{2}\mathbf{E}^{h}-\alpha\mathbf{n}\times\left(\mathbf{H}^{h}-\mathbf{H}^{h,+}\right)\right). \end{split}$$

We then have that the discrete analogue of (9) holds, establishing the stability of the method. The proof exactly mimics the standard arguments in [11].

B. Second Order Formulation

To approximate (2) we propose a generalization of the so-called energy-DG method introduced for the scalar wave equation in [12]. (The original method could be directly applied in the absence of charges by reformulating as the standard wave equation.) In energy-DG methods we introduce a new variable **weakly** equal to the time derivative of some quantity. In this setting we impose, again for polynomial test and trial functions,

$$\int_{\Omega_j} \frac{1}{\mu_0} (\nabla \times \phi_E) \cdot \left[\nabla \times \left(\frac{\partial \mathbf{E}^h}{\partial t} - \mathbf{V}^h \right) \right] =$$

$$\int_{\partial \Omega_j} \frac{1}{\mu_0} (\nabla \times \phi_E) \cdot (\mathbf{n} \times \mathbf{V}^* - \mathbf{n} \times \mathbf{V}^h),$$

$$\int_{\Omega_{j}} \epsilon_{0} \phi_{V} \cdot \left(\frac{\partial \mathbf{V}^{h}}{\partial t} + \chi * \frac{\partial \mathbf{V}^{h}}{\partial t} \right) + (\nabla \times \phi_{V}) \cdot \left(\frac{1}{\mu_{0}} \nabla \times \mathbf{E}^{h} \right) =$$

$$- \int_{\Omega_{j}} \phi_{V} \cdot \frac{\partial \mathbf{J}}{\partial t} + \int_{\partial \Omega_{j}} \phi_{V} \cdot \left(\left(\frac{1}{\mu_{0}} \nabla \times \mathbf{E} \right)^{*} \times \mathbf{n} \right).$$

A general parametrization of the fluxes is given by

$$\left(\frac{1}{\mu_0} \nabla \times \mathbf{E}\right)^* = (1 - \alpha) \left(\frac{1}{\mu_0^+} \nabla \times \mathbf{E}^{h,+}\right) + \alpha \left(\frac{1}{\mu_0^-} \nabla \times \mathbf{E}^{h,-}\right) - \beta (\mathbf{n}^+ \times \mathbf{V}^{h,+} + \mathbf{n}^- \times \mathbf{V}^{h,-}),$$

$$\mathbf{V}^* = \alpha \mathbf{V}^{h,+} + (1 - \alpha) \mathbf{V}^{h,-}$$

$$- \tau \left(\frac{1}{\mu_0^+} (\nabla \times \mathbf{E}^{h,+}) \times \mathbf{n}^+ + \frac{1}{\mu_0^-} (\nabla \times \mathbf{E}^{h,-}) \times \mathbf{n}^- \right),$$

with $0 \le \alpha \le 1$ and, if upwinding is desired, $\beta, \tau < 0$.

With these choices a discrete analogue of (11) holds, establishing the stability of the method. See [13] for details.

IV. LOCAL DISPERSION MODELS

Although our analysis only relies on the assumptions on $\hat{\chi}$ listed above, memory-efficient implementations are possible if $\hat{\chi}(s)$ is a rational function. Of course this is always the case for the standard Lorentz and Debye models, and recently a generalization (GDM) has been proposed in [14]. However, other dispersion models are also relevant, for example the general Havriliak-Negami relation with non-integral α , β [15]:

$$\hat{\chi} = \frac{\delta}{(1 + (\eta s)^{\alpha})^{\beta}},\tag{12}$$

Here we propose a generalized rational approximation based on continued fractions, which have proven to be convenient for constructing local, high-order radiation boundary conditions [16]–[19]. As motivation for this we note the following three facts:

i. All kernels satisfying (6) take the form [10]:

$$s\hat{\chi}(s) = \chi_0 + \int_{-\infty}^{\infty} \frac{\sigma(d\lambda)}{s + i\lambda},\tag{13}$$

where $\chi_0 \geq 0$ and σ is a finite measure. Such functions are also sometimes called Markov functions. The standard Lorentz-Debye and the generalized GDM models of [14] correspond to Dirac measures.

ii. A continued J-fraction

$$\hat{f}(s) = \chi_0 + \frac{\omega_0^2}{s + \gamma_1 + \frac{\omega_1^2}{s + \gamma_2 + \dots}},$$
 (14)

with $\gamma_j \geq 0$ is positive definite, converges to a function satisfying (13) and, when truncated, satisfies the Kramers-Kronig relations [20, Ch. IV, XII].

iii. Away from singular points the diagonal Padé approximant to (13) (with respect to the Laurent series) is exponentially convergent away from singularities and, for real χ , has the form (14) [21].

Our proposal, then, is to model (or approximate) $s\hat{\chi}(s)$ by a finite continued fraction in the form (14). Then, just as in the auxiliary differential equation approach of [3], [14], the pointwise polarizations in our Galerkin methods can be computed by solving a number of auxiliary differential equations. Precisely, suppose (14) is truncated after m terms. That is, the last term in the continued fraction is $\frac{\omega_{m-1}^2}{s+\gamma_m}$. We then can write, where $\mathbf{w}=\mathbf{E}^h$ for our DG discretization of (1) and $\mathbf{w}=\mathbf{V}^h$ for our DG discretization of (2),

$$\chi * \frac{\partial \mathbf{w}}{\partial t} = \chi_0 \mathbf{w} + \psi_1, \qquad (15)$$

$$\frac{d\psi_j}{dt} + \gamma_j \psi_j = \omega_{j-1}^2 \psi_{j-1} - \psi_{j+1},$$

where we set

$$\psi_0 = \mathbf{w}, \quad \psi_{m+1} = 0.$$

It is always possible to transform between the continued fraction and GDM forms, assuming that the GDM describes a kernel satisfying (6). Recall the GDM form is

$$s\hat{\chi} = \sum_{j=1}^{m} \frac{a_{0,j}s + a_{1,j}s^2}{b_{0,j} + b_{1,j}s + s^2}.$$
 (16)

To go from (16) to (14) one first writes the rational function explicitly as a ratio of polynomials and then applies the division algorithm described in [20, Ch. IX]. The calculations are always explicit. Note that such a procedure would provide a test that the proposed GDM satisfies (6). To go from (14) to (16) requires computing the poles of the rational function. These are the eigenvalues of the tridiagonal matrix with diagonal elements $-\gamma_j$, superdiagonal elements -1, and subdiagonal elements ω_j^2 .

The advantage of the GDM method is that it encompasses the standard models in current use. However, we believe our proposed form could be useful in automatically developing stable approximations. For example, one can construct rational interpolants or least squares approximations using experimental data or formulas such as (12) using the large s Padé approximants of [21]. Here we note the stable interpolation and approximation algorithms based on barycentric forms [22], [23], which can be directly transformed to the continued fraction form and monitored for stability as discussed above. These approximations can be made more efficient, that is using smaller values of m, via the application of reduced order modeling techniques such as balanced truncation, which has been successful in constructing efficient approximations to radiation boundary conditions [24], [25]. We note the work in [26] where accurate approximations to (12) are incorporated into the Yee scheme. There the short time singularity was handled using a local quadrature, but we also suspect that with appropriately chosen interpolation nodes efficient rational approximations can be constructed [27].

V. A NUMERICAL EXAMPLE

As a simple illustration we present the results of a numerical experiment using the upwind ($\alpha=1$) DG discretization of (1) mentioned above. Examples using the new energy-DG method will appear elsewhere. The problem solved is inspired by but different than the one presented in [1]. Here we look at a transverse magnetic wave in two space dimensions. The setup is a waveguide with PEC boundaries and a width of 2500nm. A metal strip of width 50nm and $\epsilon_{0,\text{metal}}=2.75\epsilon_{0,\text{vacuum}}$ is placed in the guide and a current source with a Gaussian spatio-temporal profile centered at t=5 with a temporal width $t_w=0.77$ and frequency $\omega=4.9$ and a spatial width of $r_w=200$ nm is used to excite the waves. It is centered in the middle of the waveguide a distance of 1250nm to the left of the strip. (Time is measured in femtoseconds.)

$$J_z = e^{-((t-t_0)/t_w)^2 - (r/r_w)^2} \sin(\omega(t-t_0)).$$

The dispersion model, though reasonably scaled, does not correspond to a model of a particular metal, but could be produced by a Drude-Lorentz combination. The parameters are:

$$\omega_0 = 2$$
, $\omega_1 = .715$, $\omega_2 = .65$
 $\gamma_1 = 0.1$, $\gamma_2 = 0.016$, $\gamma_3 = 0$.

We use square elements of side 25nm and compare results using tensor product polynomials of q = 3, 5, 7 in each coordinate direction for the spatial discretization in each element. Time stepping is by the standard fourth order Runge-Kutta method with $\Delta t = 1/300$, $\Delta t = 1/600$ and $\Delta t = 1200$. The domain is truncated by complete radiation boundary conditions with 5 auxiliary fields as described in [19]. These are located 2500nm to the left and 50nm to the right of the strip. In Figure 1 we plot the transmitted and reflected fields at points in the middle of the waveguide 200nm to the left and 25nm to the right of the strip respectively. Note that the source excites a variety of modes so the profiles are not as simple as would be produced by plane wave incidence. Using the q = 7 results as a reference solution we find that the reflected wave at the recording station has a maximum relative error of 1.1×10^{-5} when q = 3 and 5.1×10^{-9} when q = 5.

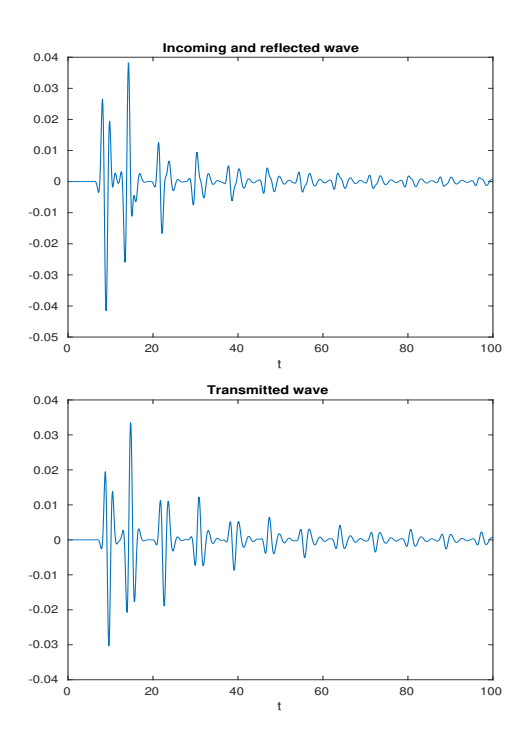


Fig. 1. Transmitted and reflected waves in the numerical experiment.

ACKNOWLEDGMENTS

This work was supported in part by NSF Grants DMS-1913076 and DMS-2012296. Any opinions, findings, conclusions or recommendations expressed in this material are those of the authors and do not necessarily reflect the views of the National Science Foundation.

REFERENCES

- Q. Ren, H. Bao, S. Campbell, L. Prokopeva, A. Kildeshev, and D. Werner, "Continuous-discontinuous Galerkin time domain (CGTD) method with generalized dispersive material (GDM) model for computational photonics," *Optics Express*, vol. 26, no. 340410, 2018.
- [2] T. Hagstrom, "Hermite methods for electromagnetic waves in dispersive media," in ACES 2019, no. 978-0-9960078-8-7, 2019.

- [3] J. W. Banks, B. Buckner, W. Henshaw, M. Jenkinson, A. Kildeshev, G. Kovacic, L. Prokopeva, and D. Schwendeman, "A high-order accurate scheme for Maxwell's equations with a Generalized Dispersive Material (GDM) model and material interfaces," *J. Comput. Phys.*, vol. 412, no. 109424, 2020.
- [4] J. Kozdon, L. Wilcox, T. Hagstrom, and J. W. Banks, "Robust approaches to handling complex geometries with Galerkin difference methods," *J. Comput. Phys.*, vol. 392, pp. 483–510, 2019.
- [5] T. Hagstrom, J. W. Banks, B. B. Buckner, and K. Juhnke, "Discontinuous Galerkin difference methods for symmetric hyperbolic systems," *J. Sci. Comp.*, vol. 81, pp. 1509–1526, 2019.
- [6] J. W. Banks, B. B. Buckner, T. Hagstrom, and K. Juhnke, "Discontinuous Galerkin Galerkin differences for the wave equation in second-order form," SIAM J. Sci. Comp., 2021, to appear.
- [7] L. Zhang, D. Appelö, and T. Hagstrom, "Energy-based discontinuous Galerkin difference methods for second-order wave equations," *Commun. Appl. Math. and Comp.*, 2021, to appear.
- [8] D. Appelö, L.Zhang, T. Hagstrom, and F. Li, "An energy-based discontinuous Galerkin method with tame CFL numbers for the wave equation," 2021, submitted.
- [9] G. Gripenberg, S.-O. Londen, and O. Staffans, Volterra Integral and Functional Equations, ser. Encyclopedia of Mathematics and its Applications. Cambridge: Cambridge Univesity Press, 1990, vol. 34.
- [10] A. Tip, "Linear dispersive dielectrics as limits of Drude-Lorentz systems," Phys. Rev. E, vol. 69, no. 016610, 2004.
- [11] J. Hesthaven and T. Warburton, Nodal Discontinuous Galerkin Methods, ser. Texts in Applied Mathematics. New York: Springer-Verlag, 2008, no. 54.
- [12] D. Appelö and T. Hagstrom, "A new discontinuous Galerkin formulation for wave equations in second order form," SIAM J. Num. Anal., vol. 53, pp. 2705–2726, 2015.
- [13] D. Appelö, T. Hagstrom, A. Petersson, and L.Zhang, "An energy-based discontinuous Galerkin method for Maxwell's equations in curl-curl form," 2021, in preparation.
- [14] L. Prokopeva, J. Borneman, and A. Kildishev, "Optical dispersion models for time-domain modeling of metal-dielectric nanostructures," *IEEE Trans. on Magnetics*, vol. 47, pp. 1150–1153, 2011.
- [15] Y. Kalmykov, W. Coffey, D. Crothers, and S. Titov, "Microscopic models for dielectric relaxation in disordered systems," *Phys. Rev. E*, vol. 70, no. 041103, 2004.
- [16] T. Hagstrom and S. Hariharan, "A formulation of asymptotic and exact boundary conditions using local operators," *Appl. Numer. Math.*, vol. 27, pp. 403–416, 1998.
- [17] S. Asvadurov, V. Druskin, M. Guddati, and L. Knizherman, "On optimal finite difference approximation of PML," SIAM J. Numer. Anal., vol. 41, pp. 287–305, 2003.
- [18] T. Hagstrom and T. Warburton, "Complete radiation boundary conditions: minimizing the long time error growth of local methods," SIAM J. Numer. Anal., vol. 47, pp. 3678–3704, 2009.
- [19] T. Hagstrom and J. Lagrone, "Complete radiation boundary conditions for Maxwell's equations," in ACES 2020, no. 978-1-7335096-0-2, 2020.
- [20] H. S. Wall, Analytic Theory of Continued Fractions. New York: D. Van Norstrand Company, 1948.
- [21] A. Aptekerov, V. Buslaev, A. Martínez-Finkelshtein, and S. Suetin, "Padé approximants, continued fractions, and orthogonal polynomials," *Russian Math Surveys*, vol. 66, pp. 1049–1131, 2011.
- [22] C. Schneider and W. Werner, "Some new aspects of rational interpolation," *Math. Comp.*, vol. 47, pp. 285–299, 1986.
- [23] Y. Nakatsukasa, O. Séte, and L. N. Trefethen, "The AAA algorithm for rational approximation," SIAM J. Sci. Comput., vol. 40, pp. A1494– A1522, 2018.
- [24] J.-R. Li, "Low order approximation of the spherical nonreflecting boundary condition for the wave equation," *Linear Alg. and its Applic.*, vol. 415, pp. 455–468, 2006.
- [25] B. Citty and T. Hagstrom, "Radiation boundary conditions for the wave equation with variable coefficients," 2021, in preparation.
- [26] M. Causley, P. Petropolous, and S. Jiang, "Incorporating the Havriliak-Negami dielectric model in numerical solutions of the time-domain Maxwell equations," J. Comput. Phys., vol. 230, pp. 3884–3899, 2011.
- [27] L. N. Trefethen, Y. Nakatsukasa, and J. A. C. Weideman, "Exponential node clustering at singularities for rational approximation, quadrature, and PDEs," *Numer. Math.*, vol. 147, pp. 227–254, 2021.